Applied Energy xxx (xxxx) xxx–xxx

Contents lists available at ScienceDirect

Applied Energy

journal homepage: www.elsevier.com/locate/apenergy

A comparison of radial-flow and axial-flow packed beds for thermal energy storage☆

J.D. McTigue[a,1], A.J. White[b,*]

[a] National Renewable Energy Laboratory, 15013 Denver West Parkway, Golden, CO 80401, USA
[b] Cambridge University Engineering Department, Trumpington Street, Cambridge CB2 1PZ, UK

HIGHLIGHTS

- Packed-bed thermal stores where the heat transfer fluid travels radially are described.
- A thermodynamic model is proposed and the stores are analysed with 2nd Law methods.
- Radial-flow stores exhibit lower pressure losses than corresponding axial-flow stores.
- Thermo-economic optimisation indicates they have competitive round-trip efficiencies.

ARTICLE INFO

Keywords:
Thermal energy storage
Packed beds
Heat transfer
Exergetic loss
Optimisation

ABSTRACT

Packed-bed thermal reservoirs are an integral component in a number of electrical energy storage technologies. The present paper concentrates on packed beds where the heat transfer fluid travels along the radial co-ordinate. The governing energy equations and various mechanisms that cause exergetic losses are discussed. The radial-flow packed bed is compared to a dimensionally similar axial-flow packed bed. This approach provides a fair assessment of the underlying behaviour of the two designs. Multi-objective optimisation allows a wide range of design variables to be considered, and is employed to compare optimal radial-flow and axial-flow stores. Axial-flow stores that have been segmented into layers are also considered. The results indicate that radial-flow stores have a comparable thermodynamic performance, but that the additional volume required for by-pass flows leads to higher capital costs.

1. Introduction

Since the late 20th century there has been a surge in the deployment of renewable energy technologies driven by concerns about anthropogenic climate change, the health impacts of particulate pollution, and diminishing fossil fuel reserves. In 2015, 7.0% of the UK's energy consumption came from renewable sources (up from 5.2% in 2011) [1]. However, to meet the 2009 EU Renewable Directive target, the UK will have to increase renewable energy deployment from around 64 TWh to approximately 230 TWh (for heat, transport and electricity) by 2020 [2]. Fig. 1 shows the predicted capacities of several renewable sources in 2020 and indicates the additional investment in renewable energy that is required. By implementing these changes, it is forecast that around 30% of UK electricity will come from renewable sources [2].

The intermittent nature of renewables creates problems for the electrical grid such as congestion, frequency and voltage control, and balancing of supply and demand. Energy storage, interconnection, and demand side management have the potential to combat these problems, and it is widely accepted that storage will form an essential component in future energy systems [3]. For example, one estimate for the UK is that, over the next few decades, integration of intermittent power sources will require storage capacities of the order of hundreds of GWh – an order of magnitude greater than current capacity [4].

1.1. Packed-bed thermal energy storage

A wide range of energy storage technologies exists and comprehensive reviews can be found in [5,6]. This paper focusses on "sensible heat" thermal energy storage (for electrical applications) in packed beds which comprise cylindrical containers filled with a solid storage

☆ The short version of the paper was presented at ICAE2016 on Oct. 8–11, Beijing, China. This paper is a substantial extension of the short version of the conference paper.

* Corresponding author.
E-mail addresses: JoshuaDominic.McTigue@nrel.gov (J.D. McTigue), ajw36@cam.ac.uk (A.J. White).

[1] This work was completed and written up while the author was affiliated with Cambridge University Engineering Department.

http://dx.doi.org/10.1016/j.apenergy.2017.08.179
Received 20 January 2017; Received in revised form 29 July 2017; Accepted 19 August 2017

Nomenclature

CAES	compressed air energy storage
CSP	concentrating solar power
LAES	liquid air energy storage
PHES	pumped hydro energy storage
PTES	pumped thermal energy storage

Greek Symbols

α	packed bed diffusivity, see Eq. (9) ($m^2\,s^{-1}$)
χ	round-trip exergetic efficiency
ΔT	maximum temperature difference, $T_d - T_c$ for a cold store (K)
Γ	dimensionless packed bed charge period, t_c/τ
Λ	dimensionless packed bed length, L/ℓ
ϕ	aspect ratio H/D for axial-flow stores, $H/2(r_o - r_i)$ for radial-flow stores
Π	dimensionless cycle period (or utilisation), $t_c/t_N = \Gamma/\Lambda$
ρ	density ($kg\,m^{-3}$)
τ	packed bed time scale, see Eq. (8) (s)
θ	fractional exit temperature
ε	packed bed void fraction

Roman Symbols

$\dot{m}$	mass flow rate ($kg\,s^{-1}$)
ℓ	packed bed length scale, see Eq. (7) (m)
St	Stanton number, $h/(Gc_{p,g})$
B	exergy (J)
C	capital cost (£)
c	specific heat capacity ($J\,kg^{-1}\,K^{-1}$)
C_B	capital cost per exergy output (£/ kWh)
C_f	friction coefficient
D	diameter of the packed bed (m)
d_p	particle diameter (mm)
e	specific internal energy ($J\,kg^{-1}$)
F	unsteady gas terms
G	mass flow rate per unit area ($kg\,m^{-3}\,s^{-1}$)
H	height of the packed bed (m)
h	heat transfer coefficient ($W\,m^{-2}\,K^{-1}$)
h_g	specific internal enthalpy ($J\,kg^{-1}$)
k	cost factors
k_{eff}	effective conductivity ($W\,m^{-1}\,K^{-1}$)
L	length of gas flow path. H for axial-flow stores, $r_o - r_i$ for radial-flow stores (m)
N_{seg}	number of segments
p	pressure ($N\,m^{-2}$)
$r_{i,o}$	radius of the inner/outer plenum (m)
S_v	particle surface-area-to-volume ratio $6/d_p$ (m^{-1})
T	temperature (K)
t_c, t_N	charging duration, nominal (fully charged) time (s)
V	volume (m^3)
V_f	thermal front velocity, see Eq. (2) ($m\,s^{-1}$)

Subscripts

c,d	charging, discharging
	gas, solid
p,i,PV	packing, insulation, pressure vessel

medium such as pebbles or gravel. Energy is transferred to the solid by means of a heat transfer fluid. Packed beds are considered to be an attractive storage option as the materials are abundant and relatively cheap. Unlike other bulk electricity storage systems, such as Pumped Hyrdo Energy Storage (PHES) or most forms of Compressed Air Energy Storage (CAES), packed beds have no geographical constraints. Further details on thermal energy storage materials and technologies can be found in [7–9].

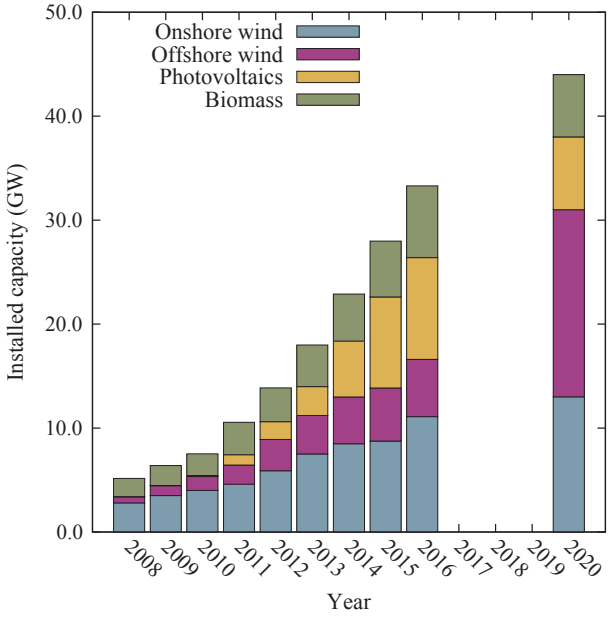

Fig. 1. Installed capacity of various renewable energy sources in the UK. Figure taken from [10]. Values at 2020 are predicted capacities from [1] and are subject to uncertainty (for instance, solar photovoltaics could vary between 7 and 20 GW).

Packed-bed thermal stores may be stand-alone components, such as in heating applications, or part of wider systems, including Concentrated Solar Power (CSP)[11,12], Advanced Adiabatic Compressed Air Energy Storage (AA-CAES), Liquid Air Energy Storage (LAES) and Pumped Thermal Energy Storage (PTES). For example, in LAES systems, the discharge phase involves compressing and heating the liquid air before expanding it through a turbine. Storing the available energy of the cold air in a packed bed prior to expansion reduces the work required to liquefy the air during the following charge cycle and substantially increases round-trip efficiency [13]. In PTES systems all of the stored energy is in the form of "thermal exergy" in either hot or cold stores or both. A heat pump is used to transfer heat from the cold to the hot store during charge and the cycle is reversed and operated as a heat engine to discharge the stores and retrieve electrical work [14–17]. Finally, cold-storage packed beds may also be used in domestic and industrial cooling systems [18,19].

In the above applications, the proposed packed bed designs are normally of the axial-flow variety. However, as discussed in more detail below, there are a number of potential advantages to radial-flow configurations, including "self insulation" and the possibility of mitigating the conflict between heat exchange and pressure losses. The purpose of the current paper is therefore to compare axial- and radial-flow designs using a consistent modelling approach in order to assess their relative merits.

Previous studies have indicated that the behaviour of packed beds can have a significant impact on overall system performance. Furthermore, the shape and thickness of the "thermal fronts" (described further below) depends on history of operation, thus requiring transient methods for accurate modelling. Models that resolve the individual (and often conflicting) loss-generating processes are required so that designs may be optimised. Consequently, an accurate evaluation of different storage technologies (such as PTES and AA-CAES) requires

detailed modelling of the packed bed behaviour. Such models should capture the time-varying behaviour of the stores, as well as evaluating thermodynamic metrics and economic factors.

This study follows previous work undertaken at Cambridge University Engineering Department [10,14,15,20,21,22] in which PTES systems were considered for electrical load shifting. A nominal PTES design was formulated in [15] with a capacity of 16 MWh, and a discharging power of 2 MW. For ease of comparison, the packed beds in the current paper have the same energy capacities as in this nominal PTES design. The focus here is mainly on the cold reservoirs because these demonstrate more clearly the trade-offs between different loss components, but similar trends are also observed in hot reservoirs.

The rest of the paper is organised as follows. An overview of axial-flow packed beds, including segmented stores is provided in section 1.2, followed by a historical literature review of radial-flow packed beds in Section 1.3. The governing equations for radial-flow packed beds are presented in Section 2, and exergetic loss mechanisms are described. The governing equations are formulated such that the assumptions and solution methods are identical to those used for axial-flow stores. In Section 3 the underlying behaviour of radial-flow stores is compared to dimensionally similar axial-flow stores using the same metrics. In Section 4 multi-objective optimisation of the packed-bed design is used to consider economic factors and the influence of a range of design variables. Together these methods provide a thorough and fair comparison of radial-flow and axial-flow stores.

1.2. Axial-flow packed beds

Investigations of packed-bed thermal energy storage typically assume that the heat transfer fluid flows axially along a cylindrical store. However, a number of innovative design features have been suggested with the aim of improving the heat transfer characteristics. For instance, Zanganeh et al. [11] developed a conical container which reduced the effect of thermal ratcheting, and also investigated the impact of incorporating phase change materials into the store [23,24].

Crandall and Thatcher [25] developed another design feature known as *segmentation* as a way to maintain thermal stratification in packed beds for solar air heating systems. Segmented stores were subsequently developed by Isentropic Ltd. for PTES systems [26] with the additional aim of alleviating the inherent conflict between heat transfer irreversibility and pressure loss. Fig. 2 illustrates one possible implementation of a segmented (layered) store where each segment is individually gated (with valves B, C and D shut, as shown). Since each layer is independently controlled, the gas flow can be directed into only those segments where the thermal front is present – i.e. where heat transfer is occurring and there are thus significant temperature gradients. The flow is diverted around the remaining segments thereby reducing pressure losses. This allows smaller particles to be used, which in turn reduces heat transfer losses. White et al. [21] examined the extent to which this improved performance, taking into account both thermodynamic and cost factors. Broadly, loss reduction is most significant when the gas density is low (which for the PTES system considered was in the cold, unpressurised store) but other factors are also important and simplified guidelines are given in the appendix of Ref. [21].

Optimisation studies indicated that segmented stores could be cheaper and/or more efficient than unsegmented ones [21,22], but these studies did not include the additional cost of valves and control systems.

1.3. Radial-flow packed beds

Fig. 3 shows a schematic of a radial-flow packed bed in which gas enters a chamber in the centre of the cylindrical container before flowing radially outward through the bed and exiting through an outer plenum. The packing material is contained by a grid through which the gas can flow. Various aspects of these packed beds have been studied, including the effective conductivity [27,28], flow distributions [29] and applications in air filters [30,31] and the synthesis of ammonia [32,33]. Models typically include reaction terms and mass transfer, and the emphasis of these papers tends to be on the chemical conversion efficiency.

Compared to axial-flow packed beds relatively little has been published on radial-flow systems for energy storage. This study describes a thermodynamic model that is appropriate for storage applications. For electrical energy storage particular consideration must be given the heat transfer processes and available energy (or exergy) losses. As shown in Fig. 4, the thermal front travels outward along the radius during charge and returns inward during discharge.

Radial-flow packed beds were first proposed for thermal energy storage in 1942 by Bradley [34]. In this patent, the thermal store heated input air to 1030 °C to be used in a blast furnace for smelting iron ore. Bradley suggested that particles of different sizes could be used. The gas velocity decreases along the radius, such that pressure losses are lowest at the outer plenum. Smaller particles can then be placed near the outer plenum in order to reduce thermal losses. Grids would have to be installed at intervals along the radius to keep particles in their respective positions.

Two further patents [35,36] in the 1990s aimed to make Bradley's concept more practicable. It was thought that the packing material might flow with the gas into the inner and outer plena. Thermal expansion could cause disintegration of the rocks, damage to the containment, or non-uniformities in the packing structure. Fassbinder's [35] and Emmel et al.'s [36] patents provided specific design features to tackle these problems. A subsequent patent [37] described a system for converting thermal energy into mechanical work which specifically used radial-flow thermal stores.

Daschner et al. [39] carried out experimental work on Emmel et al.'s design and described experimental results from a 80 kWh, 235 kW packed bed that was operated between 710 °C and 50 °C. The store achieved a first law thermal efficiency of 92%. The gas flows from the inside of the packed bed to the outside. Since the exit flow will always be close to ambient temperature, the design has so-called 'self-insulating' behaviour and should require less insulation. However, the need for an inner and outer plenum may compromise the energy density.

The inner plenum should be sized to maintain a uniform flow distribution [30], and here is set to $r_i/r_o = 0.2$. For comparison, Bradley's patent [34] suggested a system with $r_i = 5$ feet (1.52 m), $r_o = 10$ feet

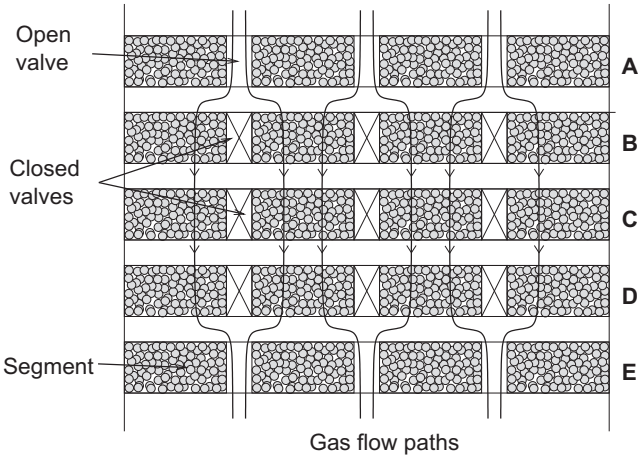

Fig. 2. Schematic of a segmented packed bed. Gas follows the path of least frictional resistance. The gas flows through the open valve in the segment A, and is then diverted through the packed bed in segments B–D due to the closed valves. Once the segment B is sufficiently charged, the valve may be opened such that gas passes through only segments C and D.

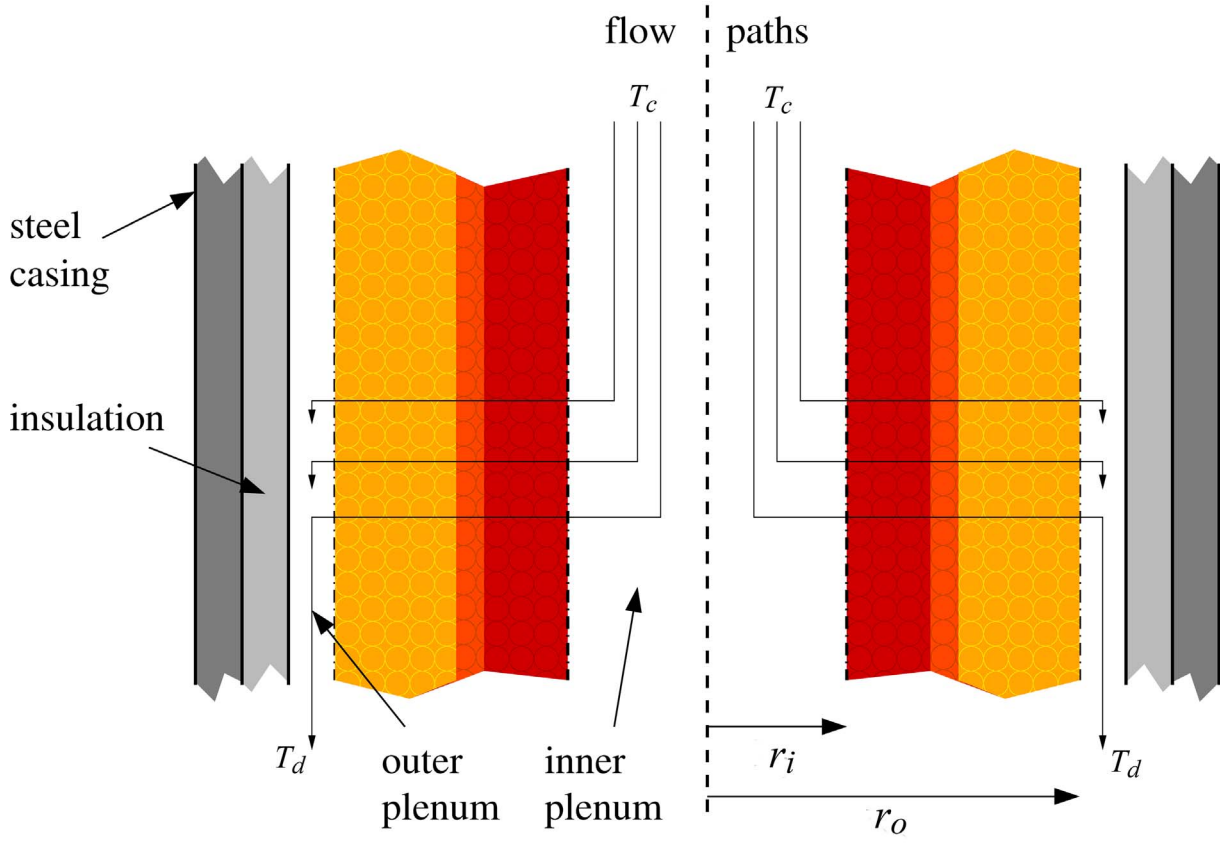

Fig. 3. Schematic of a hot radial-flow packed bed during charge. Hot gas enters the inner plenum at the charging temperature T_c and flows radially though the bed from r_i to r_o and into the outer plenum at the discharging temperature T_d.

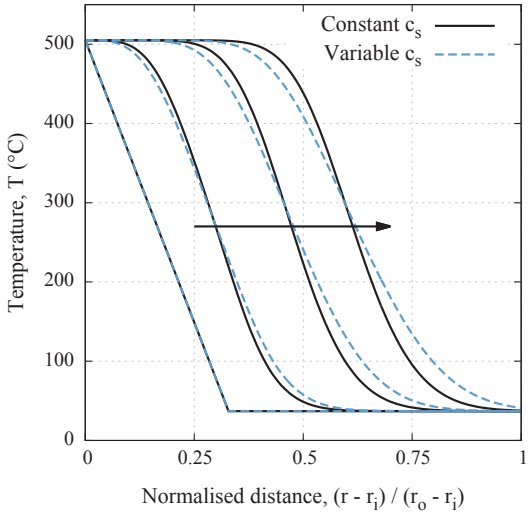

Fig. 4. Thermal front steepening due to decreasing mass flow rate per unit area G in a hot radial-flow packed bed during the first charging period. Fronts are shown at 0%, 20%, 40% and 60% of the time to fully charge the store. The impact of a variable specific heat capacity c_s is also shown, and displays spreading of the thermal front [38].

(3.05 m), meaning that $r_i/r_o = 0.5$. The prototype developed by Daschner et al. [39] used $r_i = 200$ mm and $r_o = 850$ mm such that $r_i/r_o = 0.24$.

2. Governing equations

The performance of thermal reservoirs is controlled by a number of heat transfer mechanisms, including convective heat transfer between the gas and solid, conduction along the packed bed, and heat leakage from walls of the container. Each of these processes contributes to exergetic losses – i.e., a reduction in the energy that can be recovered from the packed beds and converted to useful work. The exergetic losses and energy density are both closely related to the shape of the thermal front which is the region in the store where the temperature changes – i.e. where heat transfer occurs, as shown in Fig. 4.

The model used to quantify the heat transfer processes is based on the well-established Schumann model [40], which assumes that the flow is one dimensional, and that the internal thermal resistance of the particles is negligible. The packing is assumed to be composed of uniformly sized, spherical pebbles, which are characterised by an average equivalent diameter, d_p. The presence of the wall leads to variations in the packing structure. Consequently, the void fraction is around 0.3–0.4 in the centre of the bed, and increases to 1.0 as the wall is approached. The increased void fraction can lead to a higher velocity 'by-pass flow' which affects the heat transfer behaviour. However, these variations are typically only seen within five particle diameters of the wall, and it has been suggested that radial non-uniformities can be neglected for values of $D/d_p > 40$ [41]. In this study, D/d_p is of the order of 100. One-dimensional models such as these have been shown to give good agreement to experimental data [11,42].

The mass continuity equation is given by

$$\varepsilon \frac{\partial \rho_g}{\partial t} = -\frac{1}{r}\frac{\partial (rG)}{\partial r} \tag{1}$$

where ε is the void fraction, ρ_g is the gas density, r is the radial position, and G is the mass flow rate per unit area. Argon is used as the heat transfer fluid, and for such a gaseous working fluid it is reasonable to assume that mass accumulation is small. As a result, the mass flow rate

is roughly constant, and the mass flow rate per unit area G therefore decreases with radius as $G = G_i r_i/r$ where G_i is the mass flow rate per unit area at the inlet radius r_i. As a result, the thermal front speed V_f (which can be found from an energy balance [20]) is also a function of radius

$$V_f = \frac{c_{p,g} G_i r}{\rho_s c_s (1-\varepsilon) r} \tag{2}$$

where $c_{p,g}$ is the gas specific heat capacity, c_s is the solid specific heat capacity and ρ_s is the solid density. The velocity of the thermal front therefore decreases as it proceeds along the radius, leading to a change in the front length as shown in Fig. 4 for an initially linear front in a hot store. When the specific heat capacity c_s is constant, the front steepens up during charge. The wave speed also depends on the solid specific heat capacity which typically increases with temperature. This leads to spreading of the front [38] which counteracts the steepening caused by radial position to some extent. Since the thermal front shape changes are undone during the discharging phase, wave steepening is not as prominent in cyclic operation as it is in the single-blow case. However, changes in the front length lead to increased exergetic losses [38].

By assuming steady flow through an infinitesimal layer of a packed bed the energy equations for the gas and solid phases are expressed as

$$\varepsilon \frac{\partial}{\partial t}(\rho_g e_g) + \frac{1}{r}\frac{\partial}{\partial r}(r G h_g) = (1-\varepsilon) S_v h (T_s - T_g) \tag{3}$$

$$\rho_s c_s (1-\varepsilon)\frac{\partial T_s}{\partial t} = S_v h (1-\varepsilon)(T_g - T_s) + \frac{1}{r}\frac{\partial}{\partial r}\left(r k_{\text{eff}} \frac{\partial T_s}{\partial r}\right) \tag{4}$$

where e_g is the gas specific internal energy, h_g is the gas specific enthalpy, S_v is the particle surface-area-to-volume ratio, and h is the gas-to-particle heat transfer coefficient. A number of mechanisms contribute to the heat transfer along the radius, but is modelled here by a constant conductivity k_{eff}.

Eqs. (3) and (4) may be simplified by assuming that the mass flow rate is approximately constant. Rearranging leads to

$$\frac{\partial T_g}{\partial r} = \frac{T_s - T_g}{\ell} + rF \tag{5}$$

$$\frac{\partial T_s}{\partial t} = \frac{T_g - T_s}{\tau} + \frac{\alpha}{r}\frac{\partial}{\partial r}\left(r\frac{\partial T_s}{\partial r}\right) \tag{6}$$

where ℓ is the length scale, τ is the time scale, and α is the diffusivity. F accounts for the unsteady gas accumulation term in Eq. (3). ℓ,τ and F depend on the mass flow rate per unit area, G and thus are functions of the radius and should be integrated appropriately. These variables are given by

$$\ell = \frac{1}{(1-\varepsilon) S_v \text{St}} \tag{7}$$

$$\tau = \frac{\rho_s c_s}{c_{p,g} G S_v \text{St}} \tag{8}$$

$$\alpha = \frac{k_{\text{eff}}}{\rho_s c_s (1-\varepsilon)} \tag{9}$$

$$F = \frac{\varepsilon \rho_g}{G}\frac{\partial}{\partial t}\left(\frac{p}{\rho_g c_{p,g}} - T_g\right) \tag{10}$$

where St is the Stanton number, $h/(c_{p,g} G)$. Several refinements are made to this model, including variable gas properties and temperature dependence of the solid heat capacity c_s. These additions generally have only a small effect, with the exception of the variation of c_s which significantly affects thermal front shapes and therefore the exergetic losses [38]. White et al. [21] developed a numerical scheme to solve a similar set of equations for axial-flow stores. This scheme has been adapted to the radial-flow governing equations to facilitate comparison of packed bed designs and is discussed in more detail in [10].

Under these assumptions, the momentum flux is approximately constant along the reservoir, and the pressure drop is computed in a manner analogous to that for fully developed pipe flow [20,21]. The pressure gradient is given by

$$\frac{\partial p}{\partial r} = -\frac{S_v (1-\varepsilon) G^2 C_f}{2\varepsilon^3 \rho_g} \tag{11}$$

2.1. Exergetic loss coefficients

A number of irreversible processes act to reduce the exergetic efficiency of the packed beds. These exergetic losses are defined and investigated in greater detail in [15,20,21].

(i) Thermal losses occur as the result of a finite temperature difference between the gas and solid. Steeper thermal fronts lead to increased thermal losses as a result of reduced area for heat transfer.
(ii) Pressure losses arise due to frictional effects, and the pressure is calculated with Eq. (11). There is an inherent trade-off between thermal losses and pressure losses. For instance, long packed beds and small particles reduce thermal losses at the expense of frictional effects.
(iii) Exit losses occur as the thermal fronts emerge from the exit of the reservoir. This heat is typically rejected, although it could be recovered and used in domestic heating/cooling systems.
(iv) Heat leakage occurs through the side walls and from the top and bottom of the reservoir. The losses depend on various factors such as the size of the packed beds, the thickness of the insulation and, to a lesser extent, the convective heat transfer coefficients on the inner and outer wall.
(v) Conductive losses are due to the dissipative process of conduction between the pebbles. This loss depends on the value of the effective conductivity between particles. During storage phases, the equilibration of the thermal front due to conduction reduces the stored exergy. Conductive losses are largest where the thermal front is steep and the temperature is low [21].

3. Dimensional calculations

To compare radial-flow and axial-flow stores, the packed beds are set up so that they are dimensionally similar. The dimensionless length scale $\Lambda = L/\ell$ and the dimensionless time scale $\Gamma = t_c/\tau$ are therefore matched. L is the distance the heat transfer fluid passes through, which for an axial-flow store is the height of the store H, and for a radial-flow store is $r_o - r_i$. t_c is the duration of the charging period. The reservoirs have the same volume, mass flow rates, temperatures and pressures. The packed-beds use argon as the working fluid and magnetite (Fe_3O_4) as the storage medium. The pebbles have a diameter of 0.02 m, and the

Table 1
Geometry of dimensionally similar axial-flow and radial-flow packed beds. The radial-flow store has a diameter of 7.50 m which includes the inner plenum which has a diameter of 1.50 m – i.e., $r_i/r_o = 0.2$.

	V, m^3	$\dot{m}$, kg s^{-1}	T_c, ° C	T_d, ° C	P, bar	Λ	Γ	H, m	D, m	d_p, mm
Axial-flow	127	13.7	−150	37	1.0	108	77	5.45	5.45	20
Radial-flow								3.00	7.50	16

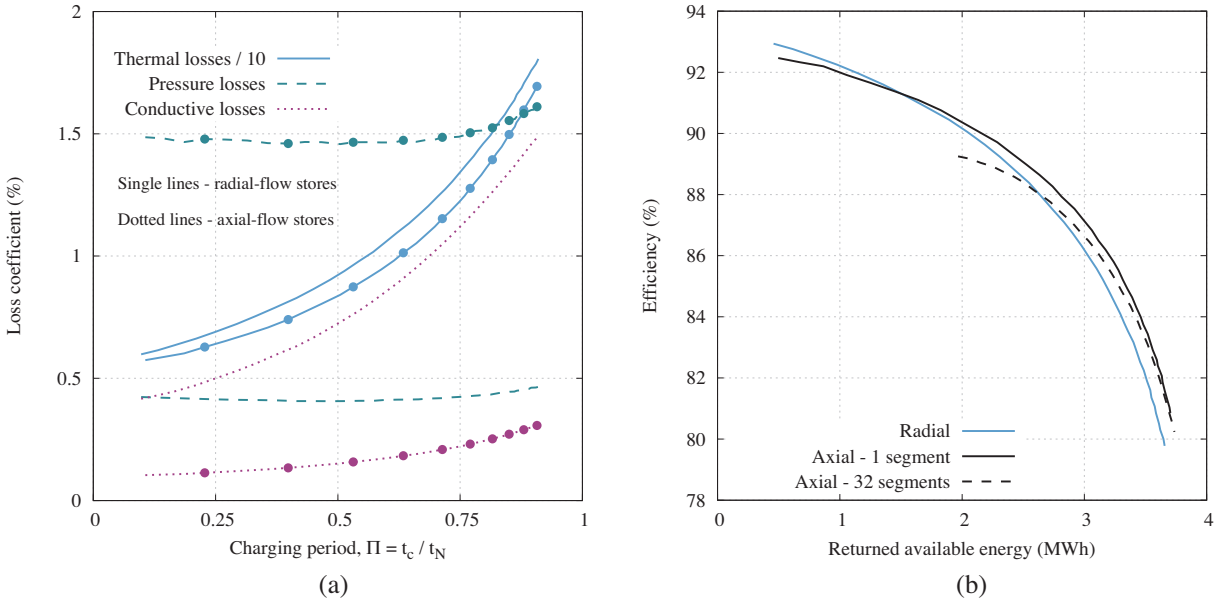

Fig. 5. Comparison of dimensionally similar cold axial-flow and radial-flow packed beds as the cycle period $\Pi = t_c/t_N$ is varied. Curves are generated by varying $\theta_{c,d}$ between 5% and 50%. (a) Lines correspond to radial-flow stores, dotted lines correspond to axial-flow stores. Note that thermal losses are 10 times larger than those displayed. (b) Trade-off between efficiency and returned available energy for radial-flow stores, axial-flow stores, and axial-flow stores that have 32 segments.

void fraction has a constant value of 0.40. The geometry of a cold axial-flow and radial-flow store are shown in Table 1 and are based on the packed beds used in a PTES system [15]. Strictly speaking, the dimensionless numbers vary with temperature and mass flow rate. For this analysis, average reservoir conditions are used to calculate the dimensionless numbers, which are then matched.

The cycle period, or utilisation, is defined as the charging time, t_c divided by the nominal time to fully charge a store, t_N such that $\Pi = t_c/t_N = \Gamma/\Lambda$. The utilisation was varied for the dimensionally similar stores and results are shown in Fig. 5. Pressure losses in the radial-flow store (single lines) are smaller than those in the axial-flow store (dotted lines) which is predominantly the result of lower gas velocities. For instance, the average G in the radial-flow store is 0.39 kg m^{-2} s^{-1}, whereas in an axial-flow store G = 0.59 kg m^{-2} s^{-1}. Furthermore, the pressure drop depends on the square of G.

On the other hand, Fig. 5a indicates that thermal and conductive losses are larger in radial-flow stores (single lines) than in axial-flow stores (dotted lines). For the same cycle period Π, a radial-flow store forms a steeper thermal front on average than in the equivalent axial-flow store. Shorter thermal fronts lead to larger thermal losses as there is a smaller area for heat transfer. In addition, the front length fluctuates due to the variation in the mass flow rate per unit area with radius. Changes in front length lead to larger thermal losses than if the front was kept at its average value [38]. Fig. 6 indicates that front lengths in radial-flow stores vary to a greater extent than in axial-flow stores. The thermal loss coefficient is calculated at each x position along the thermal fronts and is plotted in Fig. 6b which illustrates that larger thermal losses occur in radial-flow stores. In addition, steeper thermal

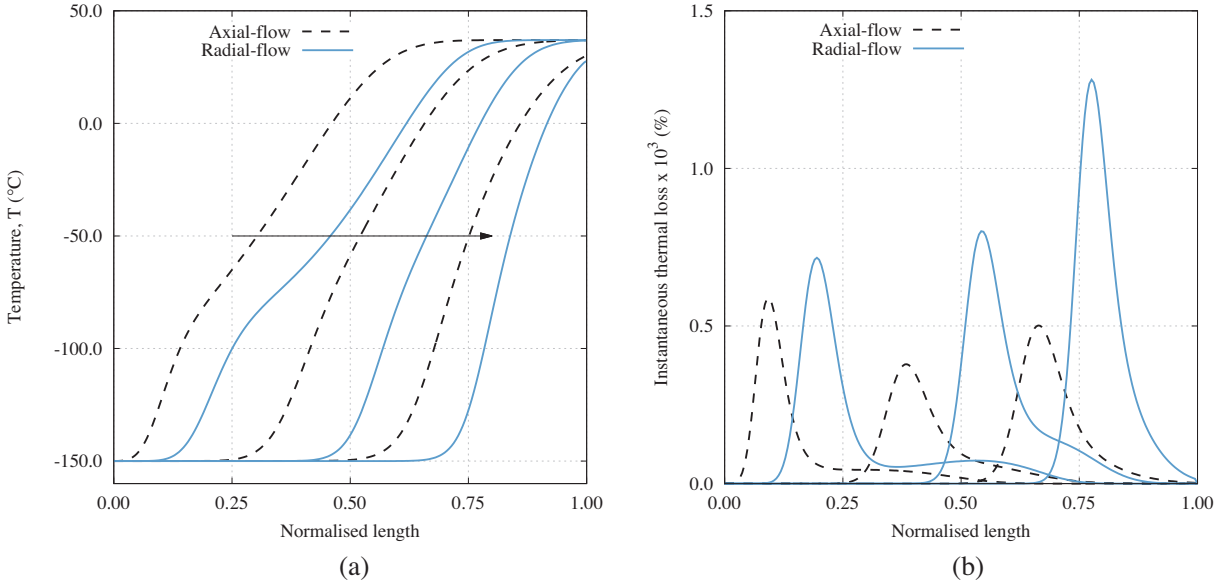

Fig. 6. Comparison of thermal fronts formed in dimensionally similar cold axial-flow and radial-flow packed beds for Π = 0.75. Profiles are plotted at t/t_c = 10%, 40% and 70% during charge. 'Normalised length' is x/H for axial-flow stores and $(r-r_i)/(r_o-r_i)$ in radial-flow stores. (a) Thermal fronts (b) Instantaneous thermal losses at each x position.

Table 2
Parameters varied during the optimisation. [a] for radial-flow stores the lower bound of ϕ is 0.1.

	ϕ	d_p, mm	θ_c, %	θ_d, %	T_c, ° C	T_d, ° C	N_{seg}
Nominal	1.0	20.0	25.0	25.0	−150.0	37.0	1
Lower bound	0.5[a]	1.5	5.0	5.0	−170.0	−170.0	1
Upper bound	2.0	20.0	50.0	50.0	37.0	37.0	32

Table 3
Cost factors used in economic analysis, see Eq. (13).

Cost factor		Value
k_p	£/m^3	1400
k_i	£/m^3	1950
k_{PV}	£/m^3 bar	200

gradients increase conductive losses.

Fig. 5b illustrates the trade-off between efficiency and returned exergy as the charging period Π is varied. Axial-flow and radial-flow packed beds that are dimensionally similar perform equally well. Radial-flow stores attain slightly higher efficiencies, but axial-flow reservoirs can store marginally more available energy. The figure also shows results for an axial-flow store with 32 segments. The segmented store can reach large energy densities but does not achieve efficiencies as high as those in the unsegmented stores. These particular segmented designs have increased thermal losses due to the process of diverting the flow into and out of the layers [21]. Previous work on axial-flow stores indicates that varying the particle diameter leads to a trade-off between thermal losses and pressure losses: smaller particle have a larger heat transfer area and lower thermal losses. However, frictional affects, and therefore pressure losses, are increased [15]. It was found that segmenting the packed beds affected this trade-off: smaller particles could be used without significantly increasing the pressure losses. This led to an overall increase in the round-trip efficiency [21]. The dimensionally similar stores in this section have the same particle diameter, so segmented stores are not able to use this advantage. However, the particle diameter is varied in the optimisation studies of section 4 which reveal the true potential of segmented stores.

The results above are representative of the differences between axial-flow and radial-flow packed beds. An exhaustive study of other factors, such as the pressure, temperatures or geometry would further emphasise the conflict between heat transfer losses and pressure losses. The influence of different parameters on these two main loss mechanisms are described in detail in appendix of Ref. [21], and also in [10,20].

4. Thermo-economic optimisation

Designing thermal reservoirs requires a number of design variables and objectives to be considered. Optimisation algorithms provide a suitable way to compare axial-flow and radial-flow packed beds. Additional factors and objectives such as economic considerations and/or volume requirements can be included.

A multi-objective optimisation algorithm known as NSGA-II [43] is employed. The decision variables are the aspect ratio ϕ, particle diameter d_p, charging temperature T_c, discharging temperature T_d and charging duration Π. Π is controlled by two parameters, θ_c and θ_d which are the fractional exit temperature T_x during which determine the end of charge and discharge. They are defined as $\theta_c = (T_x - T_d)/(T_c - T_d)$ and $\theta_d = (T_x - T_c)/(T_c - T_d)$. The parameters θ_c and θ_d are varied independently in the optimisation routine. Charge and discharge durations are therefore unequal during the first few cycles. However, once the system reaches steady-state operation, the charging and discharging periods have equal lengths. The rate of charging and discharging occurs at a constant and equal rate. Segmented stores are also optimised by allowing the number of segments N_{seg} to vary. Cold packed beds are investigated, and upper and lower limits of these variables are given in Table 2. The reservoir volume is varied in order to keep the maximum energy storage capacity constant at 11 MWh. The nominal charging time is fixed at 8 h, and the mass flow rate is calculated accordingly. This geometry is chosen to be consistent with previous investigations in [15,21].

Two objective functions are considered: the round-trip exergetic efficiency, χ and the capital cost per unit exergy returned, C_B. The efficiency is defined as the net exergy out during discharge divided by net exergy in during charge:

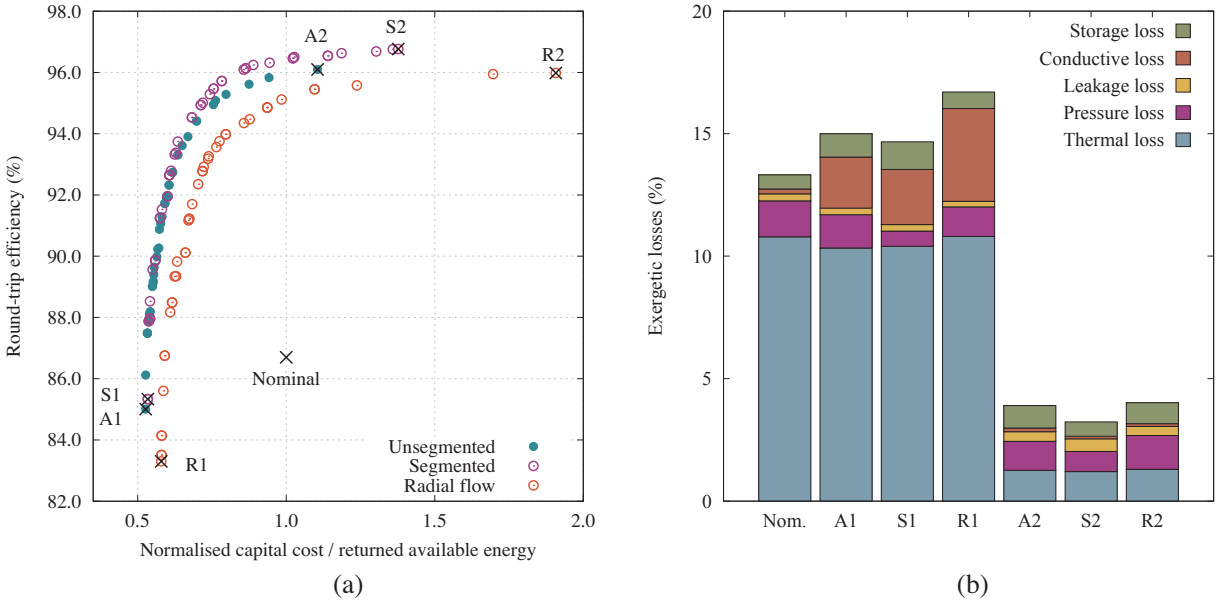

Fig. 7. Optimisation results for cold packed-bed thermal stores. 'Nominal' refers to the nominal axial-flow design in Table 1. A: unsegmented axial-flow stores. S: segmented axial-flow stores. R: radial-flow stores (a) Pareto fronts (b) Distribution of exergetic losses for the points emphasised in Fig. 7.

Table 4
Design variables and results for the optimal cold store designs that are highlighted in Fig. 7. A: axial-flow store, S: segmented axial-flow store, R: radial-flow store. χ is the round-trip efficiency, and C_B is the normalised capital cost per unit returned exergy during discharge.

		Nom.	A1	S1	R1	A2	S2	R2
ϕ		1.00	0.50	0.51	0.43	0.51	0.51	0.45
d_p	(mm)	20.0	6.0	5.6	5.9	7.5	8.1	10.7
θ_c	(%)	25.0	50.0	44.0	47.0	17.0	24.0	8.5
θ_d	(%)	25.0	50.0	49.0	50.0	9.7	18.1	17.5
T_c	(°C)	−150.0	−170.0	−170.0	−170.0	−169.7	−167.7	−165.5
T_d	(°C)	37.0	15.0	17.6	−5.1	−76.9	−114.1	−104.9
N_{seg}		1	1	9	–	1	14	–
χ	(%)	86.7	85.0	85.3	83.3	96.1	96.8	96.0
C_B		1.00	0.53	0.53	0.58	1.11	1.38	1.91

$$\chi = \frac{B_d}{B_c} \tag{12}$$

A simple model of the packed bed capital cost is used based on the material requirements of each component. The packed bed capital cost is given by

$$C = k_p V_p + k_i V_i + k_{\mathrm{PV}} V_{\mathrm{PV}} (p_o + \Delta p) \tag{13}$$

where V refers to the volume of a material, and k is the material cost per unit volume. The subscripts p,i, and PV refer to the packing material, insulation, and pressure vessel, respectively. The pressure vessel cost is proportional to the volume and pressure difference across the walls Δp. An additional term $p_o V_{\mathrm{PV}}$ allows for unpressurised vessels. Values of k are given in Table 3. More details and justification of this model are given in [10,21]. The raw capital costs are normalized by dividing it by the cost of the nominal axial flow design in Table 2. This is to avoid any misleading information being conveyed by the value of the raw cost.

Since a minimisation algorithm is used, the two objective functions f_i are formulated as

$$f_1 = 1 - \chi = 1 - \frac{B_d}{B_c} \tag{14}$$

$$f_2 = C_b = \frac{C}{B_d} \tag{15}$$

4.1. General trends in decision variables

Optimisation results for cold stores are shown in Fig. 7a as a Pareto front, which effectively demonstrates the trade-off between efficiency and cost. The Pareto front is particularly flat at high efficiencies meaning that it is possible to reduce the capital cost significantly without unduly compromising the efficiency.

C_B is reduced by either decreasing the capital cost or increasing the exergy that is returned during discharge. The capital cost is generally minimised by reducing the pressure vessel volume which for cold stores can be achieved by minimising the charging temperature T_c. Reducing T_c also improves the efficiency [10]. Conversely, T_d varies along the Pareto front as the expensive designs have a large $\Delta T = T_d - T_c$, whereas a small ΔT maximises the efficiency. However, it should be noted that integrating a packed bed into a full system may lead to constraints on the values that temperatures can take.

Fig. 7b compares the exergetic losses for the emphasised points in Fig. 7a. A design's position on the Pareto front is primarily controlled by the charging period Π; long charging durations store more energy and reduce the capital cost. However, as explained in [15,20] large Π leads to steeper thermal fronts and larger thermal losses. The optimal particle size depends on the charging periods. When a steep front is formed, smaller particles increase the heat transfer area and reduce the thermal losses. As a result, lower cost stores tend to use smaller particles, as seen in Table 4. The highest efficiency designs of A2 and R2 show the losses are more evenly distributed between thermal losses and pressure losses, at the expense of high cost due to low utilisation of the reservoir.

4.2. Comparison of optimised axial-flow and radial-flow stores

Radial-flow stores are outperformed by axial-flow packed beds. Radial-flow stores can achieve the same efficiencies as axial-flow stores but it is more expensive to do so. The high costs stem from the additional space that is required for the inner and outer plena. The inner plenum radius is 20% of the packing radius, and the outer plenum has an equal volume. If these volumes could be reduced then radial-flow stores may be comparably economical to axial-flow stores. Detailed studies are necessary to determine how small the inner plenum can be made, and what the implications on flow behaviour are. The potential improvements in radial-flow store performance could be checked by undertaking an optimisation with $r_i/r_o = 0$.

The Pareto fronts indicate that segmented thermal stores out-perform unsegmented stores: the most efficient unsegmented store is 96.2% whereas the best segmented store is 96.8%. At a fixed efficiency segmentation offers a significant cost saving. For example, the unsegmented store C4 has a normalised cost of 1.10 but for a corresponding segmented point it is around 0.87 which is roughly 20% cheaper. However, this does not include the cost of the control systems or valving, so this saving represents the amount of money that is available to be spent on additional equipment. (Note, this study does include a simple economic penalty for segmentation; bypass flow requires extra volume resulting in larger containment vessels and higher pressure vessel costs.)

The reduced pressure losses in segmented stores typically lead to larger aspect ratios and smaller particles. Consequently, the thermal fronts are steeper and the utilisation of the reservoirs increases.

5. Conclusions

This paper describes a method of storing thermal energy in a radial-flow packed bed. Such stores are relatively novel, and little has been published on using radial-flow packed beds for thermal storage applications. A framework is developed that allows a thorough and fair comparison of radial-flow and axial-flow stores. The radial geometry affects the velocity profile and thermocline shape, thereby influencing the trade-off between heat exchange and pressure losses. Radial-flow stores also provide the opportunity for "self-insulation".

The radial-flow packed bed is compared to a dimensionally similar axial-flow packed bed. Radial-flow stores typically achieve lower pressure losses, but typically exhibit steeper thermal fronts which increases thermal and conductive losses. An experimental comparison of dimensionally similar stores could improve the accuracy of these results.

Multi-objective optimization indicates that radial-flow stores have a comparable thermodynamic performance to axial-flow stores. Segmented stores were seen to have the best performance as a result of lower pressure losses and the ability to use smaller particles. In terms of

economic cost, segmented stores were the most attractive, whilst radial-flow stores were the most expensive due to the additional volume required for bypass flows. However, several uncertainties still exist in the economic modelling. Segmented store costs do not include additional internal structures, or valving and control system costs. Similarly, the size of the additional volume in the radial-flow stores is uncertain, and further work is required to determine how small it can be. Additional studies would clarify the economic arguments. Future studies could investigate the benefit of varying the particle diameter along the radius.

Acknowledgements

The work described in this paper was undertaken as part of a project funded by the UK Engineering and Physical Sciences Research Council (EPSRC Grant No. EP/J006246/1). The first author was supported by an EPSRC-funded studentship. All authors gratefully acknowledge this support.

References

[1] Digest of United Kingdom Energy Statistics (DUKES) 2015. Department of Energy and Climate Change; 2015. Available from <https://www.gov.uk/government/statistics/digest-of-united-kingdom-energy-statisticsdukes-%0A2015-printed-version>.
[2] UK Renewable Energy Roadmap Update 2012. Department of Energy and Climate Change; 2012. Available from <https://www.gov.uk/government/publications/ukrenewable-energy-roadmap-update>.
[3] Willets D. Eight great technologies. Policy Exchange; 2013.
[4] MacKay DJ. Sustainable energy - without the hot air. UIT Cambridge; 2009.
[5] Chen H, Cong TN, Yang W, Tan C, Li Y, Ding Y. Progress in electrical energy storage system: a critical review. Prog Nat Sci 2009;19(3):291–312. http://dx.doi.org/10.1016/j.pnsc.2008.07.014.
[6] Luo X, Wang J, Dooner M, Clarke J. Overview of current development in electrical energy storage technologies and the application potential in power system operation. Appl Energy 2015;137:511–36. http://dx.doi.org/10.1016/j.apenergy.2014.09.081.
[7] Sharma A, Tyagi V, Chen C, Buddhi D. Review on thermal energy storage with phase change materials and applications. Renew Sustain Energy Rev 2009;13(2):318–45. http://dx.doi.org/10.1016/j.rser.2007.10.005.
[8] Fernandes D, Pitié F, Cáceres G, Baeyens J. Thermal energy storage: how previous findings determine current research priorities. Energy 2012;39(1):246–57. http://dx.doi.org/10.1016/j.energy.2012.01.024.
[9] Gil A, Medrano M, Martorell I, Lázaro A, Dolado P, Zalba B, et al. State of the art on high temperature thermal energy storage for power generation. Part 1 concepts, materials and modellization. Renew Sustain Energy Rev 2010;14(1):31–55. http://dx.doi.org/10.1016/j.rser.2009.07.035.
[10] McTigue JD. Analysis and optimisation of thermal energy storage. PhD thesis, University of Cambridge; 2016. http://dx.doi.org/10.17863/CAM.7084.
[11] Zanganeh G, Pedretti A, Zavattoni S, Barbato M, Steinfeld A. Packed-bed thermal storage for concentrated solar power Pilot-scale demonstration and industrial-scale design. Sol Energy 2012;86(10):3084–98. http://dx.doi.org/10.1016/j.solener.2012.07.019.
[12] Bruch A, Fourmigué J, Couturier R. Experimental and numerical investigation of a pilot-scale thermal oil packed bed thermal storage system for CSP power plant. Sol Energy 2014;105:116–25. http://dx.doi.org/10.1016/j.solener.2014.03.019.
[13] Morgan R, Nelmes S, Gibson E, Brett G. Liquid air energy storage analysis and first results from a pilot scale demonstration plant. Appl Energy 2015;137:845–53. http://dx.doi.org/10.1016/j.apenergy.2014.07.109.
[14] White A, Parks G, Markides CN. Thermodynamic analysis of pumped thermal electricity storage. Appl Therm Eng 2013;53(2):291–8. http://dx.doi.org/10.1016/j.applthermaleng.2012.03.030.
[15] McTigue JD, White AJ, Markides CN. Parametric studies and optimisation of pumped thermal electricity storage. Appl Energy 2015;137:800–11. http://dx.doi.org/10.1016/j.apenergy.2014.08.039.
[16] Mercangöz M, Hemrle J, Kaufmann L, Z'Graggen A, Ohler C. Electrothermal energy storage with transcritical CO_2 cycles. Energy 2012;45(1):407–15. http://dx.doi.org/10.1016/j.energy.2012.03.013.
[17] Desrues T, Ruer J, Marty P, Fourmigué J. A thermal energy storage process for large scale electric applications. Appl Therm Eng 2010;30(5):425–32. http://dx.doi.org/10.1016/j.applthermaleng.2009.10.002.
[18] Macphee D, Dincer I. Thermal modeling of a packed bed thermal energy storage system during charging. Appl Therm Eng 2009;29(4):703–13. http://dx.doi.org/10.1016/j.applthermaleng.2008.03.041.
[19] Otanicar T, Taylor RA, Phelan PE. Prospects for solar cooling an economic and environmental assessment. Sol Energy 2012;86(5):1287–99. http://dx.doi.org/10.1016/j.solener.2012.01.020.
[20] White AJ. Loss analysis of thermal reservoirs for electrical energy storage schemes. Appl Energy 2011;88(11):4150–9. http://dx.doi.org/10.1016/j.apenergy.2011.04.030.
[21] White AJ, McTigue JD, Markides CN. Analysis and optimisation of packed-bed thermal reservoirs for electricity storage applications. Proc Inst Mech Eng Part A: J Power Energy 2016;230(7):739–54. http://dx.doi.org/10.1177/0957650916668447.
[22] McTigue JD, White AJ. Segmented packed beds for improved thermal energy storage performance. IET Renew Power Gener 2016;10:1498–505. http://dx.doi.org/10.1049/iet-rpg.2016.0031. 7.
[23] Zanganeh G, Khanna R, Walser C, Pedretti A, Haselbacher A, Steinfeld A. Experimental and numerical investigation of combined sensible latent heat for thermal energy storage at 575C and above. Sol Energy 2015;114:77–90. http://dx.doi.org/10.1016/j.solener.2015.01.022.
[24] Zanganeh G, Commerford M, Haselbacher A, Pedretti A, Steinfeld A. Stabilization of the outflow temperature of a packed-bed thermal energy storage by combining rocks with phase change materials. Appl Therm Eng 2014;70(1):316–20. http://dx.doi.org/10.1016/j.applthermaleng.2014.05.020.
[25] Crandall D, Thacher E. Segmented thermal storage. Sol Energy 2004;77(4):435–40. http://dx.doi.org/10.1016/j.solener.2003.08.011.
[26] MacNaghten J, Howes JS, Hunt RG. Improved heat storage apparatus. Patent number WO2009044139 A2; 2011.
[27] Lopez de Ramos AL, Pironti FF. Effective thermal conductivity in a packed-bed radial-flow reactor. AIChE J 1987;33(10):1747–50.
[28] Fuentes J, Pironti FF, Lopez de Ramos AL. Effective thermal conductivity in a radial-flow packed-bed reactor. Int J Thermophys 1998;19(3):781–92.
[29] Kareeri AA, Zughbi HD, Al-Ali HH. Simulation of flow distribution in radial flow reactors. Indus Eng Chem Res 2006;45:2862–74. http://dx.doi.org/10.1021/ie050027x.
[30] Heggs PJ, Ellis DI, Ismail MS. The modelling of fluid-flow distributions in annular packed beds. Gas Sep Purif 1994;8:257–64.
[31] Heggs PJ, Ellis DI, Ismail MS. Prediction of flow distributions and pressure changes in multi-layered annular packed beds. Gas Sep Purif 1995;9:243–52.
[32] Hlaváček V, Kubicek M. Modelling of chemical reactors - XXV cylindrical and spherical reactor with radial flow. Chem Eng Sci 1972;27(2):177–86.
[33] Votruba J, Hlaváček V. An experimental study of radial heat transfer in catalytic radial-flow reactors. Chem Eng J 1972;4(1):91–5.
[34] Bradley L. Regenerative stove. US patent 2 272 (108); 1942.
[35] Fassbinder HG. Regenerator. US patent 5,577,553; 1996.
[36] Emmel A, Stevanovic D, Fassbinder HG. Process for operating a regenerator and regenerator. Patent number EP 0 908 682 A2; 1999.
[37] Emmel A, Stevanovic D. Method for converting thermal energy into mechanical work. Patent number US 2004/0088980 A1; 2004.
[38] White A, McTigue J, Markides C. Wave propagation and thermodynamic losses in packed-bed thermal reservoirs for energy storage. Appl Energy 2014;130:648–57. http://dx.doi.org/10.1016/j.apenergy.2014.02.071.
[39] Daschner R, Binder S, Mocker M. Pebble bed regenerator and storage system for high temperature use. Appl Energy 2013;109:394–401. http://dx.doi.org/10.1016/j.apenergy.2012.10.062.
[40] Willmot A. Dynamics of regenerative heat transfer. Taylor & Francis; 2002.
[41] Meier A, Winkler C, Wuillemin D. Experiment for modeling high temperature rock bed storage. Sol Energy Mater 1991;24:255–64. http://dx.doi.org/10.1016/0165-1633(91)90066-T.
[42] Anderson R, Shiri S, Bindra H, Morris JF. Experimental results and modeling of energy storage and recovery in a packed bed of alumina particles. Appl Energy 2014;119:521–9. http://dx.doi.org/10.1016/j.apenergy.2014.01.030.
[43] Deb K, Pratap A, Agarwal S, Meyarivan T. A fast and elitist multiobjective genetic algorithm: NSGA-II. IEEE Trans Evol Comput 2002;6(2):182–97.